ANTIBACTERIAL PROPERTIES OF ZINC OXIDE NANOPARTICLES SYNTHESIZED BY THE SUPERNATANT OF *WEISSELLA CONFUSA* UPM22MT04

[1,2,4]A.I. AL-Tameemi [1]M.J. Masarudin. [1]R.A. Rahim. [2]V. Timms. [2]B. Neilan. [1,3]*N.M. Isa.
Lecturer Assist. Prof Prof Researcher Prof Assist. Prof.

[1]Dept. Cell and Mole. Biol. Facu. Biot and Biom Sci. University Putra **Malaysia**. [2]Scho. Env and Life Scie. University Newcastle. Australia. [3]Instit. Biosci. University Putra **Malaysia**. [4]Coll. Den. University AL IRAQIA

*Corresponding author's Email: nurulfiza@upm.edu.my

ABSTRACT

This study was aimed to produce zinc oxide nanoparticles (ZnO-NPs) using the supernatant of *Weissella confusa* UPM22MT04 and assess their effectiveness in inhibiting methicillin-resistant *Staphylococcus aureus* (MRSA). An isolate of *Weissella confusa* UPM22MT04 was isolated from a wastewater treatment plant in Johor, Malaysia, and was utilized to synthesize ZnO-NPs. The synthesized ZnO-NPs were characterized through several techniques, including UV-visible spectroscopy, Fourier-transform infrared spectroscopy, transmission electron microscopy, energy-dispersive X-ray spectroscopy, and dynamic light scattering. Monodisperse spherical ZnO-NPs of 1.7 - 7.9 nm were obtained with 0.1 M zinc nitrate at 80°C. The biosynthesized ZnO-NPs exhibited vigorous inhibitory activity against MRSA. Results found that ZnO-NPs inhibited MRSA at a minimum concentration of 0.625 mg/mL and were bactericidal at a minimum concentration of 1.25 mg/mL. In MTT assays, ZnO-NPs showed no toxicity to HS-27 fibroblasts. The supernatant of *Weissella confusa* UPM22MT04 could be used to synthesize ZnO-NPs, which are an antibacterial agent, eco-friendly and non-toxic.

Keywords: biosynthesis, *Weissella confusa*, ZnO-NPs, antibacterial activity, MRSA.

مجلة العلوم الزراعية العراقية -2023 :54(5):1209-1222 التميمي وآخرون

الخصائص المضادة للبكتريا لجسيمات أكسيد الزنك النانوية المُصنَّعة باستخدام المادة الطافية لبكتريا *Weissella confusa* UPM22MT04

احمد عيسى التميمي ماس جفري رها عبد الرحيم فيرلين تيمس بريت نيلان نورالفيزا مت عيسى
مدرس استاذ مساعد استاذ باحث استاذ استاذ مساعد

المستخلص

هدفت هذه الدراسة إلى إنتاج جزيئات الزنك النانوية (ZnO–NPs) باستخدام المادة الطافية من بكتريا *Weissella confusa* UPM22MT04 وتقييم فعاليتها المضادة للبكتيريا ضد المكورات العنقودية الذهبية المقاومة للميثيسيلين (MRSA). تم الحصول على عزلة تعود لبكتريا *Weissella confusa* من مياه الصرف الصحي في جوهور ، ماليزيا ، وتم فحصها لتخليق جزيئات الزنك النانوية. تم وصف جسيمات الزنك النانوية المركب حيوياً باستخدام مقياس الطيف المرئي للأشعة فوق البنفسجية ، تشتت الضوء الديناميكي، المجهر الإلكتروني النافذ، مطيافية الأشعة السينية المشتتة للطاقة، أطياف الأشعة تحت الحمراء باستخدام تحويل فوريه. تم الحصول على جزيئات أكسيد الزنك الكروية أحادية الانتشار (1.7–7.9) نانومتر مع نترات الزنك 0.1 مولار عند 80 درجة مئوية. النتائج اظهرت وجود تأثير مثبط قوي بواسطة جسيمات الزنك النانوية ضد MRSA ، حيث كان التركيز المثبط الأدنى من جزيئات الزنك النانوية المركب حيوياً(0.625) ملغم / مل بينما كان التركيز المبيد الأدنى من ZnO–NPs المركب حيوياً (1.25) ملغم / مل. أيضًا، لم تظهر جسيمات الزنك النانوية المركب حيوياً للدراسة أي سمية واضحة لخطوط الخلايا الطبيعية (HS–27). بشكل عام، يمكن توليف جزيئات الزنك النانوية باستخدام مادة طافية من *Weissella confusa* كعامل مضاد للبكتريا ، وهوغير سام وصديق للبيئة.

الكلمات المفتاحية: التخليق الحيوي ،*Weissella confusa* ، جسيمات الزنك النانوية، النشاط المضاد للبكتيريا، المكورات العنقودية الذهبية المقاومة للميثيسيلين.

Received:15/9/2021 Accepted:25/2/2022

INTRODUCTION

Among nosocomial infections, multidrug-resistant bacteria are the most concern to public health (13). Methicillin-resistant *S aureus* (MRSA) is one of the most common multidrug-resistant pathogens in hospitals because of its ability to survive on surfaces and its ease of transmission through skin-to-skin contact (1). Methicillin resistance is about 40-60% of *Staphylococcus aureus* samples obtained from hospitals, which is a significant concern. Furthermore, recent reports suggest that most MRSA strains are resistant to the drug vancomycin, which is one of the limited treatment options available. It has led to the emergence of vancomycin-resistant bacteria, making the situation even more alarming (30). In this regard, novel antibiotic replacement approaches should be explored and developed. It has been shown that nanoparticles, including ZnO-NP, exhibit vital antimicrobial properties (3). Among the different methods documented for producing nanoparticles, biosynthesis using probiotic bacteria has gained attention due to its low toxicity, adaptability, eco-friendliness, and efficiency. ZnO-NPs have a wide range of biological applications; hence, discovering and developing various biological systems for ZnO-NP formation is vital (20). Multiple microorganisms, such as yeast, fungi, and bacteria, can be used to produce metal nanoparticles. Probiotic bacteria, particularly their supernatant, play a significant role as antibacterial agents (37). Combining the supernatant of probiotic bacteria with other vital non-materials enhances their effectiveness against pathogens. Reaction with Zn2+, *Lactobacillus plantarum* cell biomass, and supernatant produced ZnO-NPs between 349 nm and 351 nm in size. Generally, Nanoparticles of ZnO-NPs have antibacterial properties due to the release of free Zn2+ ions, particulates of ZnO, and reactive oxygen species (22, 34). Thus, research on the antimicrobial activity of ZnO-NP synthesized by various microbes is of considerable clinical significance. *Weissella* are Gram-positive lactic acid bacteria belonging to the Leuconostocaceae family. *Weissella* strains have been found beneficial in various biotechnological and probiotic applications. For example, *Weissella* has been shown to benefit oral health, skincare, obesity, inflammatory diseases, and cancer (10, 25). The primary aim of this study was to isolate potential probiotic bacteria strains resistant to zinc. A probiotic bacteria isolate, *W. confusa* UPM22MT04, was chosen for further investigation due to its exceptional capacity for ZnO-NP synthesis. As described in this study, utilizing *W. confusa* for the biological synthesis of ZnO-NPs introduces a novel approach that expands the range of potential biotechnological applications.

MATERIALS AND METHODS

Isolation and identification of zinc-resistant potential probiotic bacteria: The study was involved to isolate probiotic bacterial isolates from samples collected from a wastewater treatment plant in Johor, Malaysia. The researchers employed a bacterial growth culture protocol to obtain zinc-tolerant probiotic bacteria. The process began with diluting one milliliter of the wastewater sample with nine milliliters of physiological saline, followed by vortexing for three minutes to achieve a uniform bacterial suspension. Next, one milliliter of the consistent bacterial suspension was added to nine milliliters of MRS broth media, then was incubated aerobically at 37°C for 48 hours. The cultured broth was serially diluted (10^{-1} to 10^{-8}) with physiological saline and inoculated onto MRS-agar plates containing 50 mg/L of zinc nitrate. The isolates were further purified by streaking them on MRS agar plates with zinc nitrate (50 mg/L) three times. The pure cultures were characterized and identified according to Bergey's Manual (5), and the Gram-positive, catalase-negative, and zinc-resistant isolates were chosen and stored in MRS broth with 30% glycerol at -80°C for future experiments.

Molecular identification of potential probiotic bacteria: Molecular identification was done by the 16S rRNA gene of the selected isolates. Following the manufacturer's instructions, genomic DNA was extracted from the potential probiotic isolates utilizing DNA Extraction Kit (BioFlux, USA), followed by amplification with specific universal primers: 27F (5′AGAGTTTGATCCTGGCTC AG-3′) and 1492R (5′GGTTACCTTGTTACGACT T-3′). For the PCR amplification, a denaturation phase of 3 minutes at 95°C was followed by

30 cycles of 30 seconds at 95°C of denaturation, followed by 30 seconds of annealing at 52°C for 30 seconds, followed by 1.30 minutes at 72°C of extension. Lastly, a 5-minute extension at 72°C was performed. The PCR products were then purified using a PCR Purification Kit manufactured by Qiagen in Germany. A Malaysian company, Apical Scientific, sequenced PCR products. Based on this process, the isolate sequences were deposited in GenBank using BLAST (www.ncbi.nlm.nih.gov/), a tool that compares genetic similarities among known strains. The next step was to retrieve closely related sequences and align them using ClustalW. Based on the maximum likelihood algorithm method with 1000 bootstrap values, the phylogenetic tree was constructed using MEGA-X software version 10.2.6 (15).

Characterization of MRSA strains

S. aureus strains (ATCC 700699 and ATCC 33742) with methicillin-resistant characteristics were collected from the Laboratory of Microbiology / Faculty of Biotechnology and Biomolecular Sciences / UPM in Malaysia. Both strains were cultured on Brain Heart Infusion agar plates and, primarily investigated with Gram staining, mannitol fermentation, catalase, coagulase, and other biochemical assays to rule out bacteria other than *S aureus* (5). *S. aureus* strains were then confirmed using the RapID STAPH (remel RapIDTM Staph Plus System, United Kingdom) assay.

Biosynthesis of ZnO-NPs using *W. confusa* UPM22MT04: A pure culture of *W. confusa* UPM22MT04 was incubated at 37°C for 18 hours in 100 mL of sterile MRS broth (Merck, Darmstadt, Germany). After that, one milliliter of 18-h-old culture previously prepared was diluted with 100 mL MRS broth and incubated at 37^{o}C for 6 h at 150 rpm shaking. After 6 hours of incubation, the optical density of the *W. confusa* UPM22MT04 suspension was measured using a UV-Visible spectrometer (Thermo Scientific), and an OD_{600} value of 1 was obtained (10). Then, by adding NaOH at a concentration of 0.4M, the pH level was adjusted to 6 to delay degradation (36). Supernatants were stored at four °C until needed after centrifugation for ten minutes at 5000 rpm to remove any bacterial cells that may present. To synthesize zinc oxide nanoparticles using *W. confusa* UPM22MT04, 5 mL of 2 M zinc nitrate was added to the flask containing 95 mL from the supernatant of *W. confusa* UPM22MT04 in a dropwise sense using magnetic stirring. The Zn(NO□)□ dissolved in water was mixed with the supernatant, leading to a concentration of Zn(NO□)□ equal to 0.1 M. Accordingly, the mixture was incubated at 80°C in a water bath for 5 to 15 minutes. The presence of white sediment at the flask's base indicates that the transformation process has occurred. Following the removal from the water bath, the flask underwent incubation for 12 hours at a temperature of 37°C (36). Under the same conditions, Zn(NO□)□ (0.1 M) and supernatant of *W. confusa* UPM22MT04 without Zn(NO□)□ were used as controls. After 12 hours of incubation, the product was centrifuged at high speed (11000 rpm) for 30 minutes to collect the ZnO-NPs. The white sediment was washed with deionized water three times to obtain dried powder, followed by a Freezer Dry System (Edwards, model RV5).

Characterization of biosynthesized ZnO – NPs : To confirm the ZnO-NPs synthesized by *W. confusa* UPM22MT04, the UV-visible spectrophotometer (Thermo Scientific, UV) was utilized to assess their optical properties within the 300-700 nm spectrum range. A UV-visible spectrophotometer of Zn(NO□)□ solutions (0.1 M) without the supernatant of bacteria was used as a control. Biosynthesized ZnO-NPs powder was dispersed in deionized water to determine the Zeta potential, polydispersity index, and particle size using dynamic light scattering (DLS, Nano-ZS from UK). The morphology and size of ZnO-NP synthesized by *W. confusa* UPM22MT04 were characterized utilizing Transmission Electron Microscopy (JEM-2100F from Japan) by suspending the ZnO-NPs powder in deionized water, putting a drop of ZnO-NPs on a grid, and air drying them. As a result, JEM-2100F (JEOL, Japan) and ImageJ software were utilized to identify the particle size and morphology of synthesized ZnO-NPs. Additionally, the arrangement of components on the exterior of the produced ZnO-NP was evaluated using Energy-dispersive X-ray

analysis (EDX, Oxford, USA) in conjunction with FE-SEM. The powder of ZnO-NPs was positioned on a stub coated with carbon film for this purpose. The surface functional groups of the produced ZnO-NPs were examined using FTIR analysis (Vector 22, Bruker, Germany) within 400 to 4000 cm^{-1}.

Determination of minimum inhibitory (MIC) and minimum bactericidal concentrations (MBC) of biosynthesized ZnO-NPs : Broth microdilution method was used to measure the MIC of the synthesized ZnO-NPs. The synthesized ZnO-NPs in powder form were mixed with sterile deionized water, and the resulting suspension was sonicated to achieve a uniform solution before usage. Different concentrations of ZnO-NP were obtained by diluting the initial stock (ranging from 2.5 to 0.039 mg/mL). MIC was identified according to Chakansin et al. (6). In summary, wells in columns 1 to 8 were filled with 100 µL of Muller Hinton broth. Subsequently, a 100 µL solution containing 5 mg/mL of biosynthesized ZnO-NPs was introduced into the first column of the microtiter plate. The solution and the medium were blended, producing a concentration of ZnO-NPs equivalent to 2.5 mg/mL. To perform the serial dilution, 100 µL of the mixture was transferred to the subsequent wells, and in the final column, 100 µL of the mixture was discarded, resulting in a final volume of 100 µL in each well. 5 µL of bacterial suspension, which had a concentration of roughly (1.5×10^8 CFU/mL) of MRSA strains, was then introduced into each well, except for the negative control. The eighth column was reserved for the positive control and contained only the bacterial suspension. Each well in row C, which had a serial dilution of nanoparticles without bacteria, was supplemented with a color/turbidity indicator (negative control). After incubation for 24 h, rows A to C of the wells were subjected to treatment with a 0.5 mg/mL resazurin solution in deionized water, utilizing a ten µL droplet, and were then subjected to a further incubation period of 4 hours at 37°C. If the color changes from blue to pink, bacteria have stimulated resazurin, and the minimum concentration of nanoparticles required to stop this color alteration of resazurin is known as MIC. After transferring a sample from the wells with MIC values to nutrient agar plates, 24-hour incubation at 37°C was conducted to determine the MBC of biosynthesized ZnO-NPs. After that, MBC was defined as a concentration where bacteria did not grow. The experiments were conducted in triplocated.

Cytotoxicity assay (MTT) of ZnO-NPs: MTT (3-[4,5-dimethylthiazol-2-yl]-2,5-diphenyltetrazolium bromide) was used *in vitro* to determine whether ZnO-NPs are cytotoxic. The HS-27 fibroblast cell line was acquired from the Cancer Research Lab at the Bioscience Institute (IBS), University Putra Malaysia. In brief, the ZnO-NP powder was blended with Dulbecco's Modified Eagle Medium and then exposed to 45W probe sonication for 5 minutes, using 3-second intervals of on and off. Subsequently, the ZnO-NPs suspension was filtered through syringe filters with 0.02 µm pores before usage. The next step involved the preparation of biosynthesized ZnO-NP concentrations ranging from 0.312 to 1.25 mg/mL. HS-27 cells were added to 96-well plates at a density of 2×10^4 (100 µL /well) in DMEM and were then incubated at 37°C with 5% CO2 for 24 hours. Next, the medium was removed, and then the cells were treated with biosynthesized ZnO-NPs (0.312, 0.652, 1.25 mg/mL) for 24 hours. Twenty-four hours after incubation, 100 µL of MTT in DMEM solution was added to each well and then incubated for an additional 4 hours at 37°C. Subsequently, a solubilization solution was applied to all wells by adding 100 µL per well of a solution comprising 10% SDS in 0.01 M HCl (30). The reactive dye was allowed to dissolve by incubating the cells at 37°C for 16 hours. The color intensity was measured using Tecan Infinite M200, Switzerland, with a reference wavelength of 570 nm). The experiments were conducted in triplicates. The formula used to calculate cell viability is as follows: Viability rate (%) = $OD_{treated}$ cells /$OD_{control}$ cells x 100

Statistical analysis

Experimental results are reported as mean ± SD. Differences between concentrations of ZnO-NPs were evaluated for significance using one-way ANOVA. A statistical

significance was indicated by a p-value of ⩽0.05.

RESULTS AND DISCUSSION

Isolation and molecular identification of zinc-resistant potential probiotic bacteria

Probiotic bacteria capable of synthesizing ZnO-NPs were isolated from samples obtained from a wastewater treatment plant in Johor, Malaysia. After screening to evaluate their resistance to zinc nitrate at a concentration of 50 mg/L, two isolates, UPM22MT04 and UPM22MT05, were chosen for further study. Various biochemical tests from Bergey's Manual of Determinative Bacteriology (5), as outlined in Table (1), were used to characterize the morphological and physiological traits of UPM22MT04 and UPM22MT05. Based on the biochemical analysis, it was found that UPM22MT04 and UPM22MT05 had rod-shaped morphology and exhibited positive results for Gram-staining but negative results for catalase activity. The molecular identification of UPM22MT04 and UPM22MT05 isolates was conducted by amplifying PCR and analyzing the sequence of their 16S rRNA. The nucleotide sequences of *W. confusa* UPM22MT04 and UPM22MT05 isolates were deposited to GenBank, NCBI (USA), and assigned accession numbers OQ102315 and OQ102316, respectively. The nucleotide sequences of UPM22MT04 and UPM22MT05, both identified as *W. confusa*, were compared to NCBI sequences by alignment. The 16S rRNA gene of UPM22MT04 and UPM22MT05 isolates share 100% similarity with that of *W. confusa* strain 3273 (MT613585.1) and *W. confusa* strain 3172 (MT613537.1), respectively, as summarized in Table (1). Meanwhile, Figure (1) exhibits the 16S rRNA study's phylogenetic tree dendrogram. As anticipated, the 16S rRNA sequences of UPM22MT04 and UPM22MT05 isolates were most closely related to identified *W. confusa* strains. *Weissella*, a Gram-positive lactic acid bacterium, belongs to the Leuconostocaceae family. It is typically present in human breast milk, saliva, vaginal discharge, feces, and fermented foods and plants (10). Studies have indicated that bacteria's ability to withstand metal ions is crucial in creating nanoparticles. Therefore, in metal stress, bacteria can transform ions into metal nanoparticles (21). In this context, it is worth noting that both isolates UPM22MT04 and UPM22MT05 of *W. confusa* exhibit remarkable resistance to zinc. These isolates can withstand high zinc levels, releasing biological substances into the surrounding supernatant and potentially participating in the synthesis of ZnO-NPs. The results of this study contribute to our knowledge regarding the range and possible uses of bacteria in the environment. Identifying zinc-resistant *W. confusa* isolates in wastewater samples emphasizes their ability to adapt and thrive in environments with high metal concentrations. Further investigation is necessary to explore their potential in nanoparticle synthesis. Interestingly, these strains of *W. confusa* also demonstrated resistance to zinc nitrate at a concentration of 50 mg/L.

Table 1. Isolation and molecular identification of probiotic bacteria isolates

Morphological characterization					Biochemical characterization		Molecular characterization	
Ordinal and GenBank Accession No.	Site of original	Source of isolates	Gram nature	Cell morphology	Catalase test	Zinc-tolerant isolate 50 mg/L	NCBI percentage similarly (100%)	Ac. No
UPM22MT04 OQ102315	Johor-Malaysia	Wastewater treatment plant	Gm+ve	rod-shaped	negative	positive	*Weissella confusa*	MT613585.1
UPM22MT05 OQ102316	Johor-Malaysia	Wastewater treatment plant	Gm+ve	rod-shaped	negative	positive	*Weissella confusa*	MT613537.1

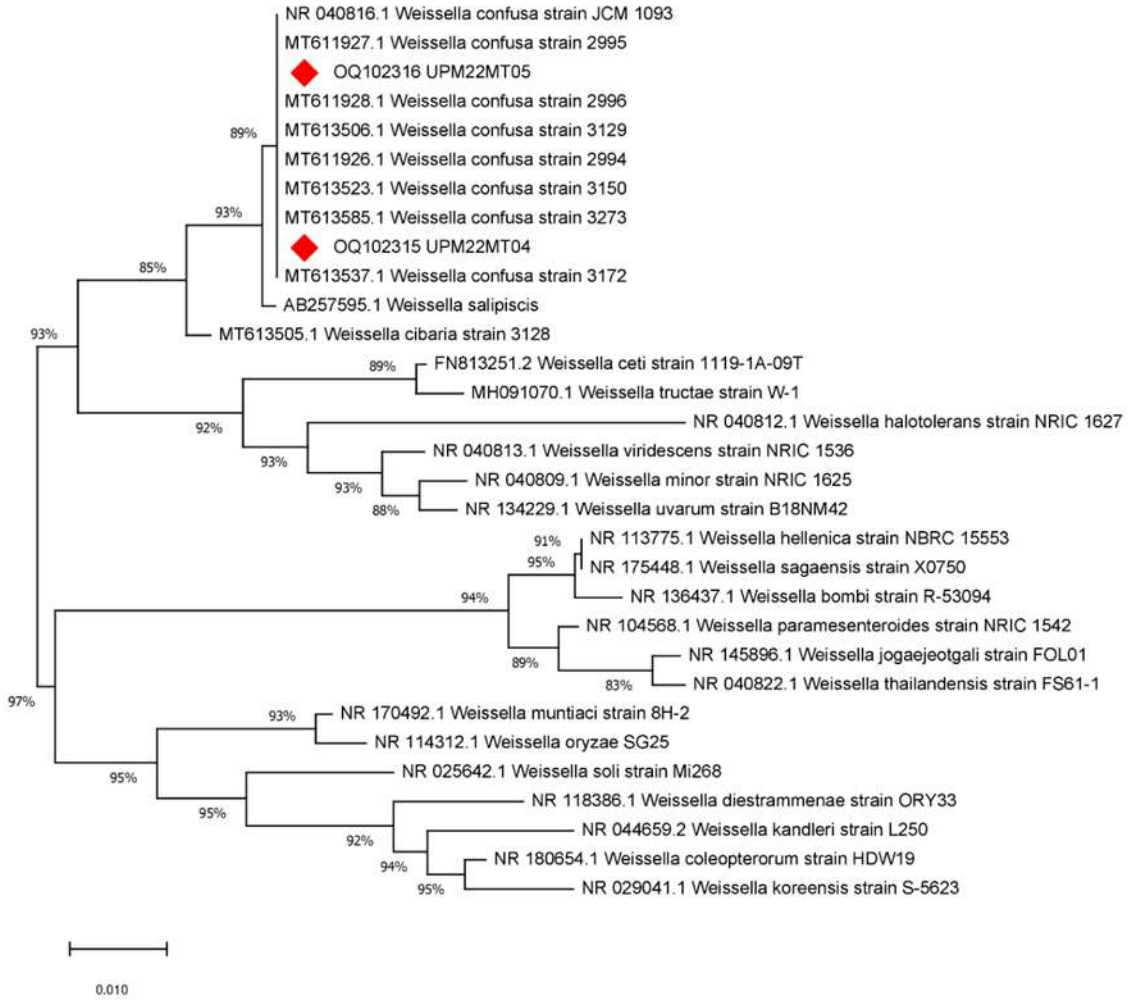

Figure 1. Using the Maximum likelihood method, a phylogenetic tree of probiotic bacterial isolates was constructed based on their 16S rRNA gene nucleotide sequences. A scale bar denotes the genetic distance. The phylogenetic tree construction was set with a bootstrap value of 1000 to replicate the confidence

Characterization of MRSA

The biochemical tests outlined in Bergey's Manual Determinative Bacteriology were employed to determine the morphological and physiological features of two MRSA strains, ATCC 700699 and ATCC 33742, as shown in Table (2). The morphological and biochemical analyses revealed that ATCC 700699 and ATCC 33742 strains displayed the characteristics of Gram-positive cocci, with the ability to ferment mannitol and positive for coagulase and catalase, while being negative for oxidase. Additionally, RapID STAPH results confirmed that both isolates belonged to the *Staphylococcus aureus* species. Skin infections were mostly caused by the staphylococcal species of *S. aureus* (1).

Table 2. Morphological and biochemical characterization of ATCC 700699 and ATCC 33742 MRSA

		Morphological characterization			Biochemical characterization			
ID Number	**Source of strains**	**Gram nature**	**Cell morphology**	**Mannitol fermentation**	**Catalase test**	**Oxidase test**	**Coagulase test**	**RapID STAPH**
ATCC 700699	**human wound**	**Gm+ve**	**Cocci-shaped**	**positive**	**positive**	**negative**	**positive**	***s. aureus***
ATCC 33742	**human wound**	**Gm+ve**	**Cocci-shaped**	**positive**	**positive**	**negative**	**positive**	***s. aureus***

Biosynthesis of ZnO-NPs using *Weissella confusa* UPM22MT04: In the present research, Zn(NO□)□ aqueous solution was reduced to ZnO-NPs when added to a supernatant extracted from *W. confusa* UPM22MT04. The production of ZnO-NPs

was initially confirmed through visual observation of the reaction between *W. confusa* UPM22MT04 supernatant and Zn(NO□)□. The formation of ZnO-NPs was indicated by white sediment at the flask's base, as shown in Figure (2-a). *W. confusa* UPM22MT04 isolate produces a high concentration by the weight of ZnO-NPs (479 mg/g) compared to *W. confusa* UPM22MT05 isolate (478.2 mg/g). So, *W. confusa* UPM22MT04 was used for the subsequent experiments. The research conducted by Selvarajan et al. (36) proposed that the negative electrokinetic potentials of bacteria aid in the swift attachment of cations, which initiates the biosynthesis process of ZnO-NPs. The functional groups of biological substances secreted by bacteria into the supernatant could facilitate the reduction of Zn(NO□)□ to ZnO-NPs. Research on the biosynthesis of ZnO-NPs has shown that the existence of functional groups, peptidoglycan, and proteins on *L. paracasei* LB3 played a significant role in reducing ZnO-NPs (14). Earlier studies have suggested that the formation of white sediment in the medium was caused by a protein secreted by the microorganism and served as a capping agent to stabilize the nanoparticles (20). Additionally, studies have indicated that bacteria's ability to withstand metal ions is crucial in creating nanoparticles. Therefore, in metal stress, bacteria can transform ions into metal nanoparticles (21). Interestingly, the *W. confusa* UPM22MT04 isolate resisted zinc nitrate at a 50 mg/L concentration. It appears that *W. confusa* UPM22MT04 can produce ZnO-NPs depending on its ability to resist Zn(NO□)□ and biological substances secreted into the supernatant.

Characterization of ZnO-NPs

UV–Visible analysis: The UV-Visible absorption spectra in Figure (2-b) displays a complete surface plasmon resonance excitation band at 335 nm, indicating the characterization of the synthesized ZnO-NPs. The peak at 335 nm is a typical characteristic of ZnO-NPS, commonly observed in such materials. As per the present investigation, the maximum absorption band is similar to that reported in previous research tudies (38).

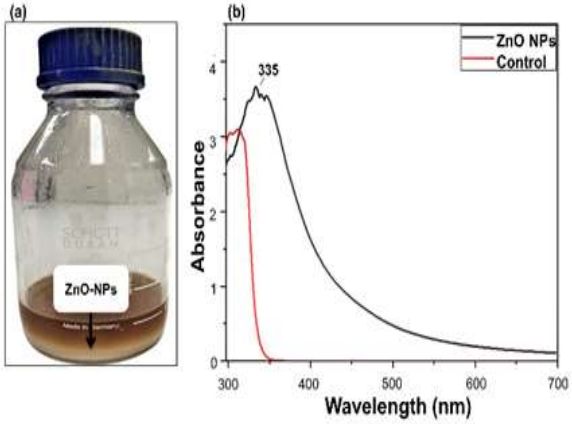

Figure 2. (a) Examining the formation of ZnO-NPs using the supernatant of *W. confusa* UPM22MT04 through visual observations. (b) UV-vis absorption spectroscopy of ZnO-NPs synthesized by supernatant of *W. confusa* UPM22MT04.

DLS analysis

As demonstrate in Figure (3-a), dynamic light scattering (DLS) analysis confirms that all particles present in the dispersion are nanoparticles, with an average size of 52.86 nm and a polydispersity index (PDI) of 0.152. The DLS analysis accounts for capping and reducing agents, resulting in a slightly larger particle size measurement than the TEM analysis (37). Apart from size, the stability of nanoparticles is also a crucial factor that impacts their biological activity (2). Zeta potential, which measures the surface charge of nanoparticles, is a commonly used parameter to assess their stability. Positive and negative zeta potential nanoparticles repel one another, preventing nano aggregation (12). If a nanoparticle exhibits a zeta potential above +30 mV or below -30 mV, it can remain stable and avoid aggregation for an extended time (28). The data shown in Figure (3-b) reveals that the average zeta potential of the synthesized ZnO-NPs was -37.1 mV, indicating that the particle is moderately stable.

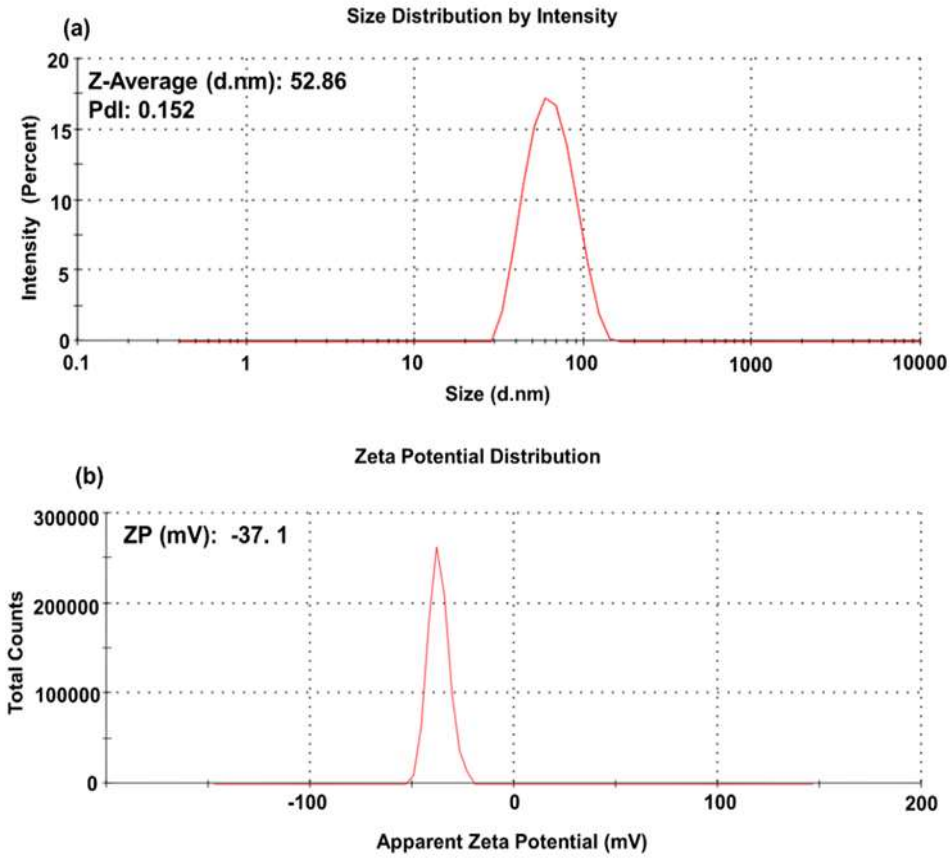

Figure 3. (a) Analysis of the particle size from ZnO-NPs synthesized by *W. confusa* UPM22MT04 (b) Zeta potential analysis of ZnO-NPs synthesized by *W. confusa* UPM22MT04

HR-TEM and EDX analysis

The High-Resolution Transmission Electron Microscopy technique investigated the morphological shapes and sizes of the ZnO-NPs synthesized using *W. confusa* UPM22MT04. At a 20 nm scale, Figure (4-a) illustrates TEM images of prepared ZnO-NPs. The ZnO-NPs observed in HR-TEM images were spherical and had different sizes. According to the HR-TEM analysis in Figure (4-b), the ZnO-NPs had an average size of 3.7 nm and a size range of 1.7 to 7.9 nm. Earlier research has suggested that the formation of nanoparticles relies on proteins secreted by microbes and acts as capping agents, thereby ensuring the stability of the NPs (19). Likewise, scientists discovered that bacteria triggered nanoparticle production by releasing an exopolymeric substance (23). The current study's formation of biosynthesized ZnO-NPs was confirmed by the EDX spectra, as shown in Figure (4-c), which displayed a zinc element peak indicating the existence of ZnO-NPs. Another element peak (Phosphorus) detected through the EDX analysis could be attributed to the broth composition (MRS) utilized for bacterial cultivation. Previous research suggests that ZnO-NPs are impure-free if the EDX analysis shows zinc and oxygen elements (7). Generally, the synthesis of ZnO-NPs obtained is too tiny without significant particle accumulation; this may be due to the proteins secreted from *W. confusa* UPM22MT04 that control nanoparticle nuclei growth and prevent accumulation, as well as the biological synthesis technique used to prepare the nanoparticles.

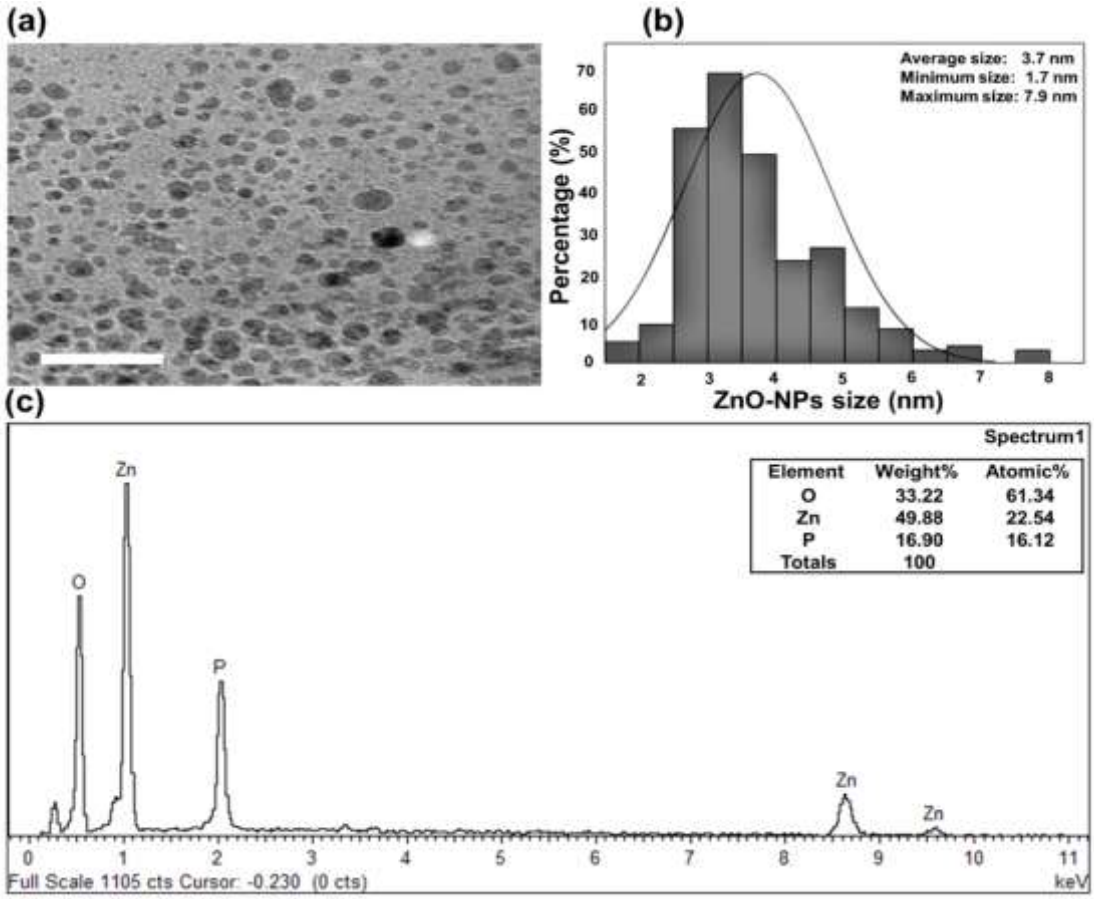

Figure 4. (a) TEM image shows biosynthesized ZnO-NPs, with a scale bar set at 20 units for reference. (b) Nanoparticle size histogram of ZnO-NPs. (c) Energy dispersive X-ray spectrum of *W. confusa* UPM22MT04 exposed to Zn^{2+}.

FTIR spectra analysis

Figure 5 illustrates the FTIR spectra acquired from ZnO-NPs synthesized using *W. confusa* UPM22MT04 supernatant. The broader peak observed at 3,219 cm^{-1} corresponds to the vibrations of the hydroxyl group (O-H) (35). Through spectral analysis, it is determined that the peaks at 1651 cm^{-1} and 1419.92 cm^{-1} signify the stretching vibration of the carbonyl group (C=O) (29, 30). Additionally, another peak observed at 1002 cm^{-1} represents the stretching vibration of the C-N bond in the amine group (39). These peaks confirm the presence of ZnO-NPs, indicated by the peaks at 420 cm^{-1}, 436 cm^{-1}, and 556 cm^{-1}, which correspond to the stretching vibrations of zinc oxide (40). The biosynthesis of ZnO-NPs using *W. confusa* UPM22MT04 supernatant involves biological substances that stabilize the NPs, preventing aggregation

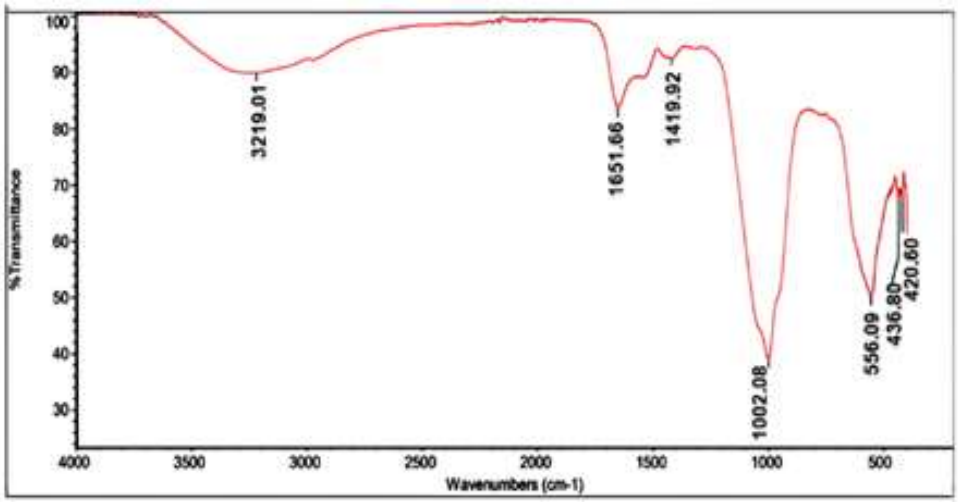

Figure 5. FTIR spectra of ZnO-NPs synthesized using *W. confusa* UPM22MT04 supernatant.

MIC and MBC determination of biosynthesized ZnO-NPs: ZnO-NPs are effective against pathogenic bacteria (3). To assess the antibacterial properties of ZnO-NPs produced by *W. confusa* UPM22MT04 on methicillin-resistant *S. aureus* strains ATCC 700699 and ATCC 33742, a turbidometric assay was used using resazurin. After incubated for 24 hours, 10 µL of 0.5 mg/mL resazurin in deionized water was added to each well and then incubated at 37°C for four hours before being ready for measurement. Based on the results in Figure 6, it was found that the lowest concentration at which the color remained unchanged for both *S. aureus* strains (column-3, rows A and B) was 0.652 mg/mL. The 'C' row data indicates that the ZnO-NPs did not cause the reduction of the resazurin dye. Live bacteria were the only ones that reduced the dye's blue tint to pink. Meanwhile, at a 1.25 mg/mL concentration, the ZnO-NPs exhibited bactericidal properties against both MRSA strains. In the previous study, ZnO-NPs were synthesized using the supernatant produced by *Pseudomonas hibiscicola* to assess its antibacterial properties. Based on the characterization study's results, it was found that biosynthesized ZnO-NPs had spherical morphologies, and *P. hibiscicola* secreted a protein that reduced, stabilized, and capped them (33). Results of the antimicrobial activity showed that synthesized ZnO-NPs were efficient against *S. aureus*. Lately, ZnO-NPs were synthesized employing *P. chrysogenum* filtrate. The characterization of the produced nanoparticles was carried out to evaluate their effectiveness against microorganisms. The results indicated that the ZnO-NPs prepared at a 2 mg/mL concentration exhibited antibacterial activity against *S. aureus* (18). Table 3 displays comparative results of the antibacterial activity of several biosynthesized ZnO-NPs. The synthesized ZnO-NPs exhibited excellent antibacterial activity against methicillin-resistant *S. aureus* compared to the others. ZnO-NPs' antibacterial activity depends on their size and concentration (41). This study showed that the biosynthesized ZnO-NPs were smaller and displayed highly effective antibacterial properties. This study focused on MRSA, which causes human wound infections. Therefore, it is possible that ZnO-NPs prepared from *W. confusa* UPM22MT04 supernatant for treating these infections can be used as a potential antibacterial agent.

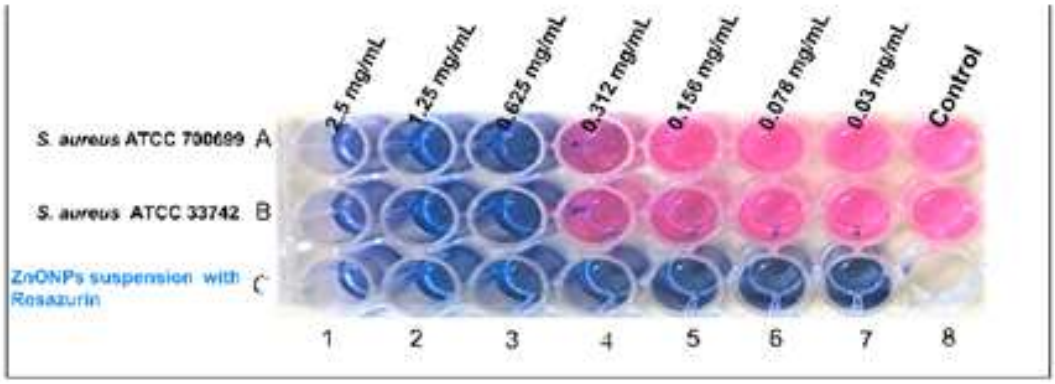

Figure 6. Resazurin microtitre assay for determining the MIC of ZnO-NPs against one of the human skin pathogens, MRSA. The eighth column was positive control and contained only the bacterial suspension. Row C was negative control and contained only a serial dilution of nanoparticles without bacteria. Blue color: no bacterial growth, pink color: bacterial growth. MIC of ZnO-NPs: 0.625 mg/mL third column.

Table 3. Comparative of earlier results with ZnO-NPs synthesized by *W. confusa* UPM22MT04 for the antibacterial activity against MRSA

Nanoparticle	Size (nm)	MIC mg/ml	Model bacteria	References
ZnO-NPs	50	4 -8	*S aureus*	(33)
ZnO-NPs	40	2.5 -5	*S aureus*	(32)
ZnO-NPs	9-35	2	*S aureus*	(18)
ZnO-NPs	1.7-7.9	0.625	*S aureus*	Present study

ZnO-NP cytotoxicity assay *in vitro*

The *in vitro* toxicity of ZnO-NPs produced through biosynthesis was evaluated at varying concentrations (1.25, 0.652, and 0.312 mg/mL) against HS-27 cells. In previous research, Meyer et al. (17) reported that ZnO-NPs could be toxic to living cells and tissues. Despite the previous research indicating the toxicity of ZnO-NPs, the biosynthesized ZnO-NPs tested in this study did not exhibit any toxicity toward normal human skin cells (HS-27), as shown in Figure 7. The cell viability (%) comparisons among treated and untreated control groups of applied different concentrations of the ZnO-NPs on HS-27 did not have statistically significant (P-Value = 0.06). The results suggest that concentrations of ZnO-NPs used in the study did not affect the viability of HS-27 cells. The non-toxic nature of the synthesized ZnO-NPs toward HS-27 cells could be attributed to the surface coating that prevented their interaction with the cells, thus reducing their toxicity. At the highest concentrations of ZnO-NPs (0.652 and 1.25 mg/mL), the viability of HS-27 cells was approximately 95% and 94%, respectively. Based on the antibacterial and cytotoxicity assessments, the ZnO-NPs at 0.652 and 1.25 mg/mL demonstrated the most potent antibacterial activity and did not exhibit any toxicity towards fibroblast cells. Nagajyothi et al. (26) reported in a prior study on biosynthesized zinc oxide nanoparticles that even at a concentration of 1 mg/mL, no toxicity was observed in RAW 264.7 cells. Similarly, Leite-Silva et al. (16) discovered that zinc oxide nanoparticles were not harmful beneath the application sites, irrespective of whether the epidermis was intact or damaged. Due to the significant barrier function of the skin, penetration of ZnO-NPs through the epidermis is infrequent, which helps prevent the entry of external substances into the epidermis (28). Blanpain et al. (4) stated that the stratum corneum primarily provides physical barriers to the skin that prevent environmental damage. The available evidence suggests that the potential for skin penetration of ZnO is low. Although the biosynthesized ZnO-NPs did not demonstrate any observable toxicity towards HS-27 cells, assessing their safety in diverse cell types and through in vivo studies before utilizing them for various applications is crucial.

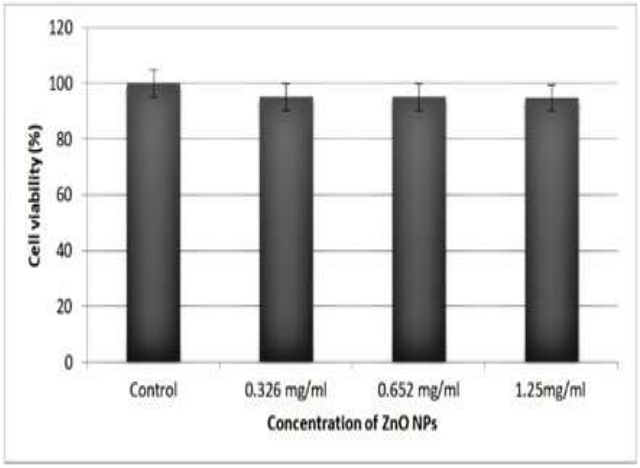

Figure 7. The survival rate of HS-27 cells exposed to varying concentrations of biosynthesized ZnO-NPs. The data represent the mean ± SD of three independent experiments.

CONCLUSION

The ability to form nanoparticles may vary among different strains of microorganisms. Also, the physicochemical characteristics of nanoparticles can vary depending on their source, which can directly impact their intended applications. Wastewater contains bacteria with high tolerance to toxic substances and enzymatic reduction ability and has the potential to be rich in species that can synthesize nanoparticles. Thus, identifying probiotic bacteria with the potential to produce nanoparticles by isolating a novel strain from wastewater sources is a promising strategy. It was confirmed that the probiotic bacterial strain utilized in the research was *W. confusa* UPM22MT04. The study discovered that *W. confusa* UPM22MT04 could generate ZnO-NPs with antibacterial characteristics against MRSA, indicating potential applications. The smaller the nanoparticle, along with accessory secretory proteins, can enhance the antibacterial properties of the nanoparticle. It was observed that the ZnO-NPs synthesized through the biological method did not exhibit any discernible toxicity toward HS-27 cells. In addition, biologically produced ZnO-NPs could provide an alternative to chemical and physical methods.

REFERENCES

1. Abd Zaid, A. M., and N. J. Kandala. 2021. Identification of methicillin resistant *Staphylococcus aureus* using touchdown PCR

and phenotypic methods from patients and hospitals environments in different Iraqi cities. Iraqi Journal of Agricultural Sciences, 52(6):1356-1364.
https://doi.org/10.36103/ijas.v52i6.1475
2. Aiad, I., M.M. El-Sukkary, E.A. Soliman, M.Y. El-Awady, and S.M. Shaban, 2014. In situ and green synthesis of silver nanoparticles and their biological activity. Journal of Industrial and Engineering Chemistry, 20(5): 3430-3439.
3. Alden, M.A. and L.A. Yaaqoob, 2022. Evaluation of the Biological Effect Synthesized Zinc Oxide Nanoparticles on *Pseudomonas aeruginosa*. Iraqi Journal of Agricultural Sciences, 53(1): 27-37. https://doi.org/10.36103/ijas.v53i1.1502
4. Blanpain, C. and E. Fuchs, 2009. Epidermal homeostasis: a balancing act of stem cells in the skin. Nature reviews Molecular Cell Biology, 10(3): 207-217.
5. Brenner, D.J., N.R. Krieg, and J.T. eds. Staley, 2005. Bergey's Manual® of Systematic Bacteriology: Volume Two: The Proteobacteria (Part C). Springer US.
6.Chakansin, C., J. Yostaworakul, C. Warin, K. Kulthong and S. Boonrungsiman, 2022. Resazurin rapid screening for antibacterial activities of organic and inorganic nanoparticles: Potential, limitations and precautions. Analytical Biochemistry, 637:114449.
7.Djearamane, S., T.H. Ravintharan, S.X.T. Liang, and L.S. Wong, 2022. Sensitivity of Proteus vulgaris to Zinc Oxide Nanoparticles. Sains Malays, 51:1353-1362.
8.El-Sayed, H.S., S.M. El-Sayed and A.M. Youssef, 2021. Novel approach for biosynthesizing of zinc oxide nanoparticles using *Lactobacillus gasseri* and their influence on microbiological, chemical, sensory properties of integrated yogurt. Food Chemistry, 365: 130513.
9.El-Shanshoury, A.E., S.E. Elsilk and P.S. Ateya, 2013. Uptake of some heavy metals by metal resistant *Enterobacter* sp. isolate from Egypt. Afr. J. Microbiol. Res, 7(23): 2875-2884.
10.Fusco, V., G.M. Quero, G.S. Cho, J. Kabisch, D. Meske, H. Neve, W. Bockelmann and C.M. Franz, 2015. The genus *Weissella*: taxonomy, ecology and biotechnological potential. Frontiers in Microbiology, 6: 155.
11.Harandi, F.N., A.C. Khorasani, S.A. Shojaosadati and S. Hashemi-Najafabadi, 2021. Living *Lactobacillus*–ZnO nanoparticles hybrids as antimicrobial and antibiofilm coatings for wound dressing application. Materials Science and Engineering: C, 130: 112457.
12. Honary, S. and F. Zahir, 2013. Effect of zeta potential on the properties of nano-drug delivery systems-a review (Part 2). Tropical Journal of Pharmaceutical Research, 12(2): 265-273.
13. Jaddoa, N.T.M. and L.A. Gharb, 2021. The antibiofilm activity of Hibiscus sabdriffaL. against methicillin resistant *staphylococcus aureus*. Iraqi Journal of Agricultural Sciences. 52(3):626-631.
https://doi.org/10.36103/ijas.v52i3.1352
14. Król, A., V. Railean-Plugaru, P. Pomastowski, M. Złoch and B. Buszewski, 2018. Mechanism study of intracellular zinc oxide nanocomposites formation. Colloids and Surfaces A: Physicochemical and Engineering Aspects, 553: 349-358.
15. Kumar, S., G. Stecher, M. Li, C. Knyaz and K. Tamura, 2018. MEGA X: molecular evolutionary genetics analysis across computing platforms. Molecular Biology and Evolution, 35(6): 1547.
16. Leite-Silva, V.R., W.Y. Sanchez, H. Studier, D.C. Liu, Y.H. Mohammed, A.M. Holmes, E.M. Ryan, I.N. Haridass, N.C. Chandrasekaran, W. Becker and J.E. Grice, 2016. Human skin penetration and local effects of topical nano zinc oxide after occlusion and barrier impairment. European Journal of Pharmaceutics and Biopharmaceutics, 104: 140-147.
17. Meyer, K., P. Rajanahalli, M. Ahamed, J.J. Rowe and Y. Hong, 2011. ZnO nanoparticles induce apoptosis in human dermal fibroblasts Via p53 and p38 pathways. Toxicology in Vitro, 25(8): 1721-1726.
18. Mohamed, A.A., M. Abu-Elghait, N.E. Ahmed and S.S. Salem, 2021. Eco-friendly mycogenic synthesis of ZnO and CuO nanoparticles for in vitro antibacterial, antibiofilm, and antifungal applications. Biological Trace Element Research, 199: 2788-2799.

19. Mohd Yusof, H., N.A. Abdul Rahman, R. Mohamad and U.H. Zaidan, 2020a. Microbial mediated synthesis of silver nanoparticles by *Lactobacillus Plantarum* TA4 and its antibacterial and antioxidant activity. Applied Sciences, 10(19): 6973.
20. Mohd Yusof, H., R. Mohamad, U.H. Zaidan and N.A. Abdul Rahman, 2019. Microbial synthesis of zinc oxide nanoparticles and their potential application as an antimicrobial agent and a feed supplement in animal industry: a review. Journal of Animal Science and Biotechnology, 10: 1-22.
21. Mohd Yusof, H., R. Mohamad, U.H. Zaidan and N.A.A. Rahman, 2020b. Sustainable microbial cell nanofactory for zinc oxide nanoparticles production by zinc-tolerant probiotic *Lactobacillus plantarum* strain TA4. Microbial Cell Factories, 19: 1-1.
22. Mohd Yusof, H., A. Rahman, R. Mohamad, U.H. Zaidan and A.A. Samsudin, 2020c. Biosynthesis of zinc oxide nanoparticles by cell-biomass and supernatant of *Lactobacillus plantarum* TA4 and its antibacterial and biocompatibility properties. Scientific Reports, 10(1): 1-13.
23. Moreno-Martin, G., M. Pescuma, T. Pérez-Corona, F. Mozzi and Y. Madrid, 2017. Determination of size and mass-and number-based concentration of biogenic SeNPs synthesized by lactic acid bacteria by using a multimethod approach. Analytica Chimica Acta, 992: 34-41.
24. Morowvat, M.H., K. Kazemi, M.A. Jaberi, A. Amini and A. Gholami, 2023. Biosynthesis and Antimicrobial Evaluation of Zinc Oxide Nanoparticles Using *Chlorella vulgaris* Biomass against Multidrug-Resistant Pathogens. Materials, 16(2): 842.
25. Mustafa, H.N. and I. Al-Ogaidi, 2023. Efficacy of zinc sulfide-chitosan nanoparticles against bacterial diabetic wound infection. Iraqi Journal of Agricultural Sciences,54(1):1-17. https://doi.org/10.36103/ijas.v54i1.1671
26. Nagajyothi, P.C., S.J. Cha, I.J. Yang, T.V.M. Sreekanth, K.J. Kim and H.M. Shin, 2015. Antioxidant and anti-inflammatory activities of zinc oxide nanoparticles synthesized using Polygala tenuifolia root extract. Journal of Photochemistry and Photobiology B: Biology, 146: 10-17.
27. Naskar, A. and K.S. Kim, 2019. Nanomaterials as delivery vehicles and components of new strategies to combat bacterial infections: Advantages and limitations. Microorganisms, 7(9): 356.
28. Nohynek, G.J., E.K. Dufour and M.S. Roberts, 2008. Nanotechnology, cosmetics and the skin: is there a health risk?. Skin Pharmacology and Physiology, 21(3): 136-149.
29. Obeizi, Z., H. Benbouzid, S. Ouchenane, D. Yılmaz, M. Culha and M. Bououdina, 2020. Biosynthesis of Zinc oxide nanoparticles from essential oil of Eucalyptus globulus with antimicrobial and anti-biofilm activities. Materials Today Communications, 25: 101553.
30. Ogunyemi, S.O., Y. Abdallah, M. Zhang, H. Fouad, X. Hong, E. Ibrahim, M.M.I. Masum, A. Hossain, J. Mo and B. Li, 2019. Green synthesis of zinc oxide nanoparticles using different plant extracts and their antibacterial activity against *Xanthomonas oryzae* pv. *oryzae*. Artificial cells, nanomedicine, and biotechnology, 47(1): 341-352.
31. Pomastowski, P., A. Król-Górniak, V. Railean-Plugaru and B. Buszewski, 2020. Zinc oxide nanocomposites—Extracellular synthesis, physicochemical characterization and antibacterial potential. Materials, 13(19): 4347.
32. Punjabi, K., S. Mehta, R. Chavan, V. Chitalia, D. Deogharkar and S. Deshpande, 2018. Efficiency of biosynthesized silver and zinc nanoparticles against multi-drug resistant pathogens. Frontiers in Microbiology, 9: 2207.
33. Rehman, S., B.R. Jermy, S. Akhtar, J.F. Borgio, S. Abdul Azeez, V. Ravinayagam, R. Al Jindan, Z.H. Alsalem, A. Buhameid and A. Gani, 2019. Isolation and characterization of a novel thermophile; *Bacillus haynesii*, applied for the green synthesis of ZnO nanoparticles. Artificial Cells, Nanomedicine, and Biotechnology, 47(1): 2072-2082.
34. Rasheed, H.T., K.J. Luti and M.A. Alaubydi, 2020. a probiotic application of *Lactobacillus acidophilus* ht1 for the treatment of some skin pathogens. Iraqi Journal of Agricultural Sciences, 51(6):1559–1571. https://doi.org/10.36103/ijas.v51i6.1183
35. Riaz, M., U. Sharafat, N. Zahid, M. Ismail, J. Park, B. Ahmad, N. Rashid, M. Fahim, M.

Imran and A. Tabassum, 2022. Synthesis of biogenic silver nanocatalyst and their antibacterial and organic pollutants reduction ability. ACS Omega, 7(17): 14723-14734.

36. Selvarajan, E. and V.J.M.L. Mohanasrinivasan, 2013. Biosynthesis and characterization of ZnO nanoparticles using *Lactobacillus plantarum* VITES07. Materials Letters, 112: 180-182.

37. Singhal, G., R. Bhavesh, K. Kasariya, A.R. Sharma and R.P. Singh, 2011. Biosynthesis of silver nanoparticles using *Ocimum sanctum* (Tulsi) leaf extract and screening its antimicrobial activity. Journal of Nanoparticle Research, 13: 2981-2988.

38. Sujatha, J., S. Asokan and S. Rajeshkumar, 2021. Antidermatophytic activity of green synthesised zinc oxide nanoparticles using *Cassia alata* leaves. Journal of Microbiology, Biotechnology and Food Sciences, 2021: 348-352.

39. Tettey, C.O. and Shin, H.M., 2019. Evaluation of the antioxidant and cytotoxic activities of zinc oxide nanoparticles synthesized using *Scutellaria baicalensis* root. Scientific African, 6: e00157.

40. Umavathi, S., M. Subash, K. Gopinath, S. Alarifi, M. Nicoletti and M. Govindarajan, 2021. Facile synthesis and characterization of ZnO nanoparticles using *Abutilon indicum* leaf extract: An eco-friendly nano-drug on human microbial pathogens. Journal of Drug Delivery Science and Technology, 66: 102917.

41. Zarei, M., A. Jamnejad and E. Khajehali, 2014. Antibacterial effect of silver nanoparticles against four foodborne pathogens. Jundishapur Journal of Microbiology, 7(1): e8720.